Preparation of nano-ZnO@polytetrafluoroethylene superhydrophobic coating and its anti-biological adhesion properties

Z. Y. Xue[a], C. Q. Li[a,*], G. Q. Xu[a], F. F. Mao[a], T. C. Mao[a], A. Amirfazli[b]
[a]*School of Materials Engineering, Jiangsu University of Technology,Changzhou 213001,China*
[b]*Department of Mechanical Engineering, York University, Toronto ON M3J 1P3, Canada*

Multifunctional superhydrophobic surfaces that are resistant to biological adhesion have great application potential in marine science, biomedicine, and food engineering. In this study, a superhydrophobic surface was prepared by a simple spraying process with blended nano-ZnO and polytetrafluoroethylene (PTFE). The prepared surface was characterized by fourier transform infrared spectroscopy (FTIR) and field emission scanning electron microscopy (FESEM), and the influence of the mass ratio of PTFE to nano-ZnO and the spraying distance on the morphology and wettability of the coating were investigated. In addition, the friction resistance of the coating and its antibacterial properties for Escherichia coli, Staphylococcus aureus, and Candida albicans were studied. Results showed that the optimal mass ratio of PTFE to nano-ZnO was 4:1 and that the optimal spraying method was spraying from near to far. SEM images indicated a compact surface structure of the surface with a thickness of about 100μm and the substrate was tightly bonded with the coating. The superhydrophobic properties of the coating surface were stable after friction testing. More importantly, the coating showed excellent antibacterial performance, which provides a reference for the research and application of superhydrophobic coatings with desirable anti-biological adhesion properties.

(Received March 23, 2023; Accepted May 15, 2023)

Keywords: Superhydrophobic, Polytetrafluoroethylene, Nano-ZnO, Antibiological adhesion

1. Introduction

The fouling and contamination of surfaces caused by biological adhesion are major challenges in daily life and industry. For example, the fouling of ships leads to corrosion and increases hydrodynamic resistance[1-3]. Microbial contamination may threaten human life safety in food and healthcare systems[4-6]. Besides, surfaces of many materials can breed corrosive mucedine in a humid environment. Superhydrophobic surfaces show great potential in solving the problem of biological adhesion because of their low contact area with water, low viscous force[7-10],

* Corresponding author: xzy17365381209@163.com
https://doi.org/10.15251/DJNB.2023.182.639

self-cleaning[11,12], anti-corrosion[13,14], anti-fogging[15], anti-icing[16,17] and oil-water separation characteristics.

The main influencing factors in constructing superhydrophobic surfaces are surface free energy and rough structure. In past decades[18,19], nano-oxides were the most widely studied materials in superhydrophobic coatings, because of their micro/nanostructure and unique characteristics. Among them, nano-zinc oxide (ZnO) is one of the most widely studied materials. It is a wide-bandgap semiconductor (3.37eV) with many desirable characteristics such as low cost, high earth crust abundance, easy morphological adjustment, excellent chemical and mechanical properties, good thermal stability, and environmental friendliness[20,21]. Most importantly, many studies have reported that nano-ZnO can inhibit the activity of organic matters and has toxicological effects on bacteria and cells[22,23]. On the other hand, polytetrafluoroethylene (PTFE) is widely used in various industrial coatings due to its surface lubricity, low surface energy, high chemical inertia, and high-temperature resistance[24]. Rahmah et al.[25] prepared a mixed superhydrophobic modified ZnO/PVC suspension with antibacterial properties using the chemical precipitation method. The superhydrophobic mixed suspension was dropped cast on the surface of the clean glass substrates to obtain a superhydrophobic coating and it showed good inhibition against Klebsiella spp. and Staphylococcus epidermidis. Mohammad et al.[26] successfully produced a PTFE superhydrophobic coating with hierarchical structure by spraying on metal surface.

Herein, γ-aminopropyl triethoxysilane (KH550) and perfluorodecyl triethoxysilane (PFTS) were respectively used to disperse nano-ZnO powder and then blended with PTFE and carbon nanotubes (CNTs). The nano-ZnO@PTFE superhydrophobic coating was successfully prepared by a simple spraying process. The microstructure of the coating was observed by a scanning electron microscope (SEM), the phase composition of the powder was analyzed by X-ray diffraction (XRD), and chemical structures of the powder and coating were characterized by infrared spectroscopic analysis. Furthermore, the mechanical, chemical, and environmental stabilities of the coating were also analyzed. Finally, the anti-protein and anti-bacterial properties were tested.

2. Experimental

2.1. Materials

Nano-ZnO powder (Guangzhou Changyu Chemical Technology Co., Ltd., China); γ-aminopropyl triethoxysilane (KH550, Nanjing Chuangshi Chemical Additives Co., Ltd., China); Perfluoro-decyl triethoxysilane (PFTS, purity ≧99.8%, Quzhou Dongye Chemical Technology Co., Ltd., China); Polytetrafluoroethylene (PTFE, Dongguan Zhanyang Polymer Materials Co., Ltd., China); Carbon nanotubes (CNTs, Suzhou Hengqiu Technology Co., Ltd., China); Analytically pure acetone (Chinasun Specialty Products Co., Ltd., China); Analytically pure ethanol (Sinopharm Chemical Reagent Co., Ltd., China); Analytically pure sodium hydroxide (Shanghai Macklin Biochemical Co., Ltd., China); 1060 pure aluminum sheet with dimensions of 5 mm × 5 mm × 1 mm (Yonghao Irondware Insulation Materials Store, China); Escherichia coli (CMCC44102, Shanghai Preservation Biotechnology Center, China); Staphylococcus aureus (CMCC26003, Shanghai Preservation Biotechnology Center, China); Candida albicans (CMCC98001, Shanghai Luwei Technology Co., Ltd., China); Phosphate buffer (PBS, Guangzhou

Hewei Medical Technology Co., Ltd., China); Rose Bengal Agar (Beijing Luqiao Technology Co., Ltd., China); LB nutritional agar (Haibo Biotechnology Company, China).

2.2. Preparation method of superhydrophobic coating

2.2.1. Pretreatment of Al substrate

The 1060 pure Al sheet was polished in different directions with 300# sandpaper and then with 1200# sandpaper to increase the adhesion between the coating and the substrate. The polished Al sheet was cleaned with ethanol under ultrasonic treatment for 30min to remove the stains. Finally, the Al sheet was washed with deionized water three times and dried for later use.

2.2.2. Preparation of nano-ZnO@PTFE superhydrophobic coating

A brief step in the preparation of nano-ZnO@PTFE superhydrophobic coating was showed in Fig. 1. 45mL ethanol/deionized aqueous solution was prepared at a volume ratio of 8:1. 4g nano-ZnO with a particle size of about 30 nm was added to the solution and stirred. Then the suspension was ultrasonicated for 30min. KH550 (mass fraction of 10% of ZnO) was dropwise added to the suspension and magnetically stirred at a constant temperature of 35℃ for 1h. Subsequently, PFTS (mass fraction of 10% of ZnO) was dropped in the liquid and magnetically stirred at 35℃ for 4h to obtain the mixed liquor A.

Acetone of the same mass was respectively added to 0, 2, 4, 6, 8, and 10g of PTFE coating, and stirred vigorously to get the PTFE solution. 0.2g carbon nanotubes were added to the PTFE solution and stirred to obtain the mixed liquor B.

The mixed liquors A and B were blended and stirred evenly. The blended liquor was sprayed onto the prepared aluminum substrate by a spray gun. The spraying distance was precisely controlled, and different spraying distances of 0.1, 0.2, 0.3, 0.4, and 0.5m were used respectively to obtain different coatings. After curing at room temperature for 24h, the samples were placed in an oven for 30min at 100℃ to obtain ZnO@PTFE superhydrophobic coatings.

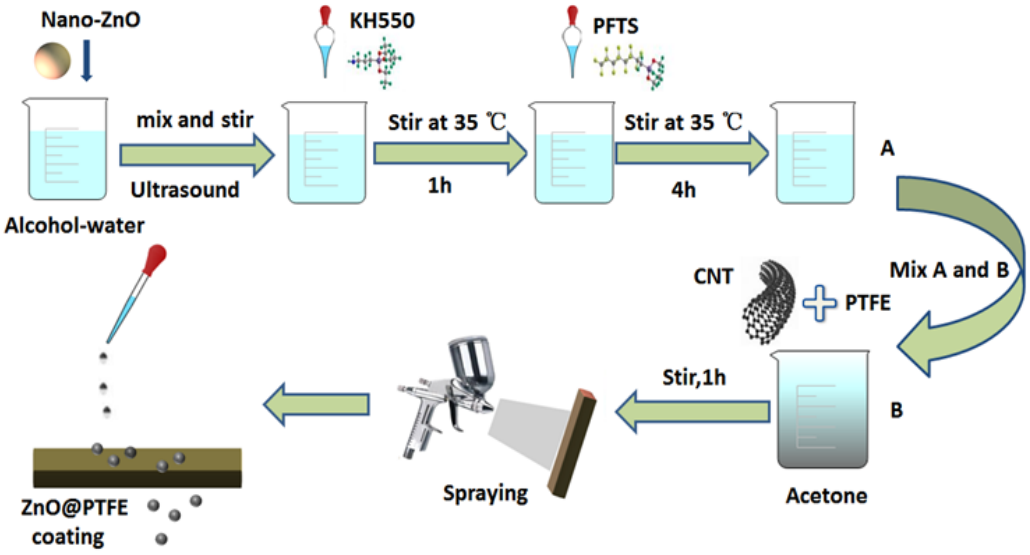

Fig. 1. Schematic illustration of the preparation process of nano-ZnO@PTFE superhydrophobic coating.

2.3. Materials characterization and performance testing

The contact angle and sliding angle of the coatings were tested by the contact angle measuring instrument. For each coating, two angles were measured three times and the average values were taken as the experimental contact angle and sliding angle. Morphologies of the coatings were characterized by high-resolution FESEM and energy dispersive spectroscopy (EDS). Fourier transform infrared (FTIR) spectroscopy was used to characterize the grafted functional groups on the powder surface and coating surface in the range of 750-4000cm^{-1}. The friction resistance of the coatings was tested by a steel velvet friction machine. The friction rod of the steel velvet friction machine was glued to the back of ZnO@PTFE coating, tightly attached to 1200 mesh sandpaper. 100g weight was loaded onto the coating, and the friction test was carried out at a speed of 2m/min. The wettability of the coating was measured when the friction rod slid by every 0.5m.

To prepare LB nutritional agar medium, 40g LB nutritional agar was dissolved in 1000mL deionized water. The agar was separated into several portions and autoclaved for 15min at 121℃ in an autoclave for later use.

To prepare Rose Bengal Agar medium, 36.6g Rose Bengal Agar was dissolved in 1000mL deionized water. The agar was separated into several portions and autoclaved for 15min at 121℃ in an autoclave for later use.

In the antibacterial test, Escherichia coli (CMCC44102), Staphylococcus aureus (CMCC26003), and Candida albicans (CMCC98001) were used as test strains, and hygienic-grade high-density polyethylene (HDPE) was used as a blank control to evaluate the antibacterial activity of the sample. First, the surfaces of coatings and control samples were wiped with 70% alcohol. After 5min, the surfaces were rinsed with deionized water and dried naturally for later use. In a sterile environment, a certain amount of the third generation of slant strains was dipped by a sterile inoculation ring and added to PBS buffer (30mL), and then the mixture was well shaken to form a homogenous solution. The coating and control sample were placed in a sterilized petri dish, and 100μL bacterial solution was respectively dipped onto the surfaces of coatings and control sample with a pipette gun. Here, the bacterial solution was fully in contact with the surfaces of the coating and the control sample, and the liquid did not overflow during the process. The petri dish was placed in an incubator for 24h at 37℃. Then the surfaces of coatings and the control sample were rinsed with PBS buffer, again immersed in a sampling cup containing PBS buffer (50mL), and shaken on a shaker for 10min to elute the bacteria. The bacteria were collected in the PBS buffer. 200μL bacterial solution was taken and diluted with 1.8mL PBS buffer to get 10^{-1} bacterial solution. 200μL bacterial solution from 10^{-1} bacterial solution was taken and diluted again in 1.8mL PBS buffer to get 10^{-2} bacterial solution. In this way, we obtained 10^{-1} to 10^{-6} bacterial solutions by diluting the original bacterial solution six times. Subsequently, 200μL of 10^{-2}, 10^{-4}, and 10^{-6} PBS bacterial suspensions were respectively dropped onto three sterilized culture media and spread evenly with a coating stick. The plates carrying the sterilized culture media were placed upside down in a constant temperature incubator (37℃) until clear colonies appeared. The number of colonies was counted by a colony counter shown in Fig. 2. For each dilution of each sample, three parallel samples were taken, and their average value was calculated as the final colony count. Fig. 2. shows the antibacterial test process and the antibacterial rate was calculated by the following formula:

$$R=(B-A)/B\times 100\% \quad (1)$$

where R (%) is the antibacterial rate, A and B are the colony counts on the coating surface and the control sample surface, respectively.

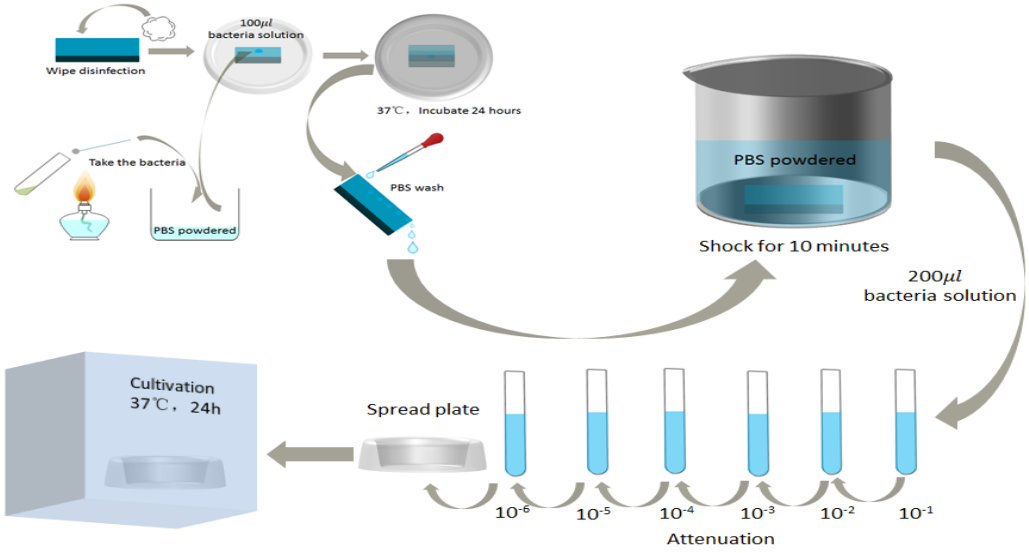

Fig. 2. Flow chart of the antibacterial test process.

3. Results and discussion

3.1. Chemical component analysis

γ-aminopropyl triethoxysilane (KH550) is a good inorganic modifier. Its surface has aminopropyl groups to endow nano-ZnO by its hydrophobic oleophilic ability and surface active sites. It improves the compatibility of nano-ZnO with the organic system and reduces the agglomeration, making the coating more compact and stable. On the other hand, halogen anions have high atomic polarity, and they can capture the electrons to form strong covalent bonds when they combine with other elements so that they are recognized as hydrophobic groups. In this research, perfluoro-decyltriethoxylsilane (PFTS) containing a large number of hydrophobic groups was used to modify ZnO nanoparticles by reducing the surface energy of the powder and increasing the hydrophobicity of the coating. Fig. 3. shows the modification mechanism of γ-aminopropyl triethoxysilane.

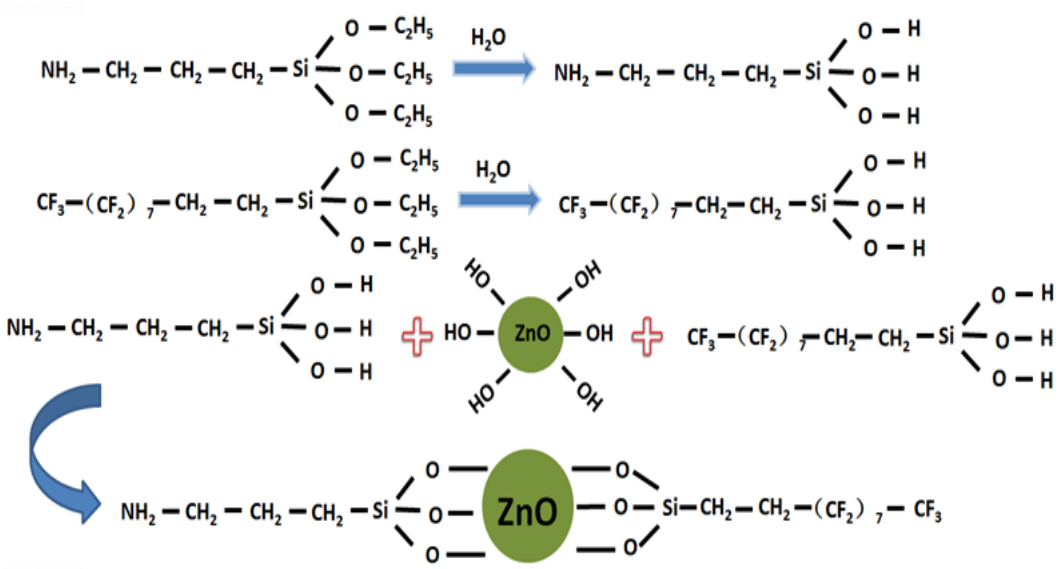

Fig. 3. The modification mechanism of γ-aminopropyl triethoxysilane.

Fig. 4. shows the infrared (IR) spectra of nano-ZnO powder before and after modification. There are -OH peaks at 3369cm^{-1} for nano-ZnO powder before and after modification, however, the intensity of the absorption peak is weakened after modification. This is attributed to the Zn-O-Si peak, generated by the dehydration condensation reaction between the hydrolysis products of KH550 and PFTS and the -OH groups adsorbed on ZnO powder surface. The peak near 2974cm^{-1} corresponds to -CH_2- stretching vibration, the peak at 1629cm^{-1} corresponds to the in-plane bending vibration of -NH_2, and two peaks at 1244 and 1145cm^{-1} are the characteristic peaks of C-F in PFTS. The peak around 1052cm^{-1} is the in-plane vibration of Si-O-Si, produced by hydrolytic polycondensation of KH550 and PFTS. This is attributed to the slower rate of dehydration condensation of the silane coupling with nano-ZnO after hydrolysis than that of polycondensation reaction or the polycondensation reaction induced by the excessive amount of silane coupling agent. In addition, there is a Zn-O-R peak at 884cm^{-1}. To sum up, infrared analysis indicates that KH550 and PFTS have been successfully grafted onto the surface of the nano-ZnO powder.

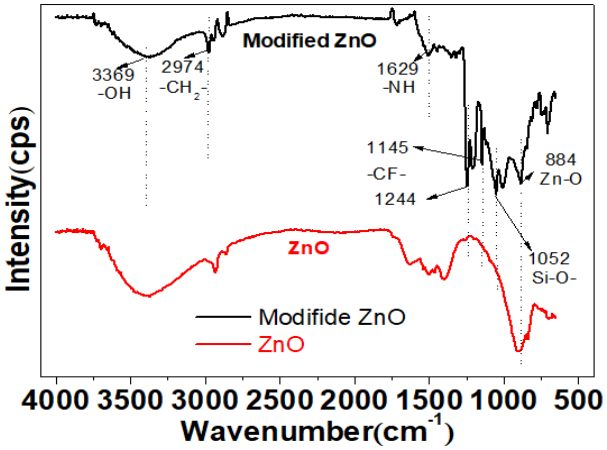

Fig. 4. IR spectra of nano-ZnO powder before and after modification.

3.2. Influences of the mass ratio of PTFE to nano-ZnO and the spraying distance

Fig. 5. shows the wettability changes with the spraying distance at different mass ratios of PTFE to nano-ZnO. For different mass ratios, the best hydrophobic performance of the coating is achieved at a contact angle of about 160° and a sliding angle of about 5°. Fig. 5(a). and b reveal that when the mass ratio of PTFE to nano-ZnO is 0:1 or 1:1, the best hydrophobic performance of the coating is achieved at any spraying distance. From Fig. 5(c), when the mass ratio increases to 2:1, the hydrophobic performance at close distances of 0.1 and 0.2m is reduced. When the mass ratio increases to 3:1, the best superhydrophobic performance is achieved only at the spraying distances of 0.4 and 0.5m (Fig. 5(d) and (e)). When the mass ratio further increases to 5:1 (Fig. 5(f)), the contact angle and sliding angle of the coating are only 150° and 10°, respectively, even at a spraying distance of 0.5m, and superhydrophobicity is not ideal. According to these results, as the mass ratio of PTFE to nano-ZnO increases, the hydrophobic performance of the coating decreases. With the increase in spraying distance, the hydrophobic performance of the coating increases.

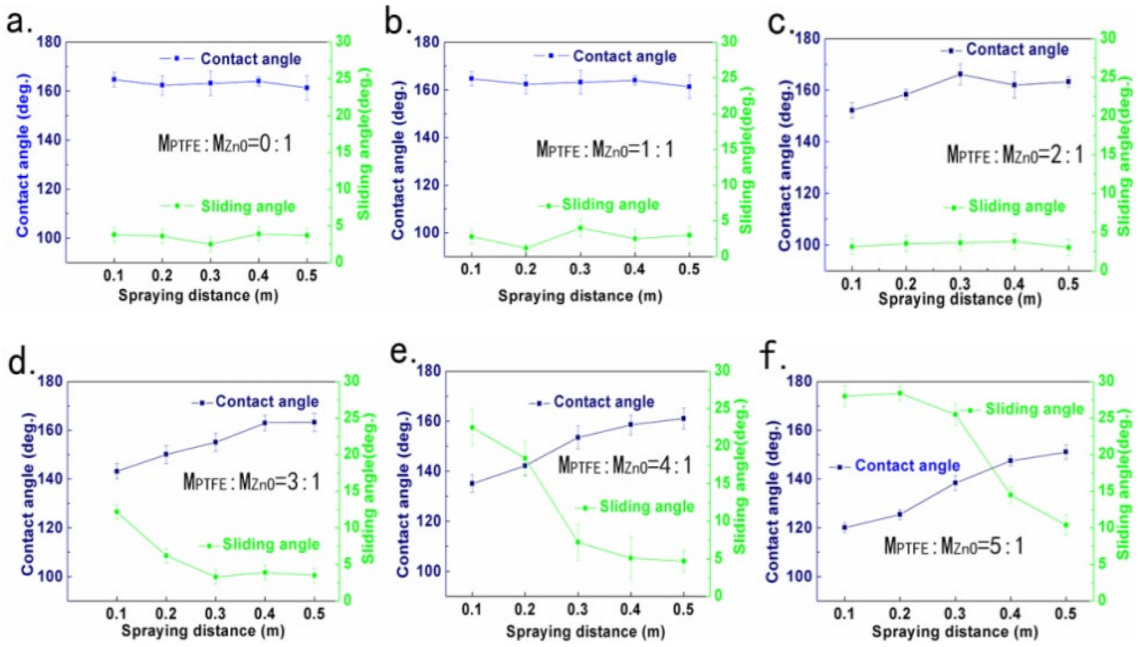

Fig. 5. Wettability of the coating at different mass ratios of PTFE to nano-ZnO; (a) MPTFE:MZnO=0:1. (b) MPTFE:MZnO=1:1. (c) MPTFE:MZnO=2:1; (d) MPTFE:MZnO=3:1. (e) MPTFE:MZnO=4:1. (f) MPTFE:MZnO=5:1.

Rough surface structure and low surface energy are necessary conditions to construct superhydrophobic surfaces. In the whole system, nano-ZnO is the main micro/nanostructure in the coating with low surface energy. When the mass ratio of PTFE to nano-ZnO is small, nano-ZnO is the main constituent of the system, and the coating shows good superhydrophobic performance, regardless of the spraying distance. With the increasing mass ratio, PTFE gradually becomes the main constituent of the system. When the spraying distance is small, the movement time is short when the system is under the atmospheric environment, and nanoparticles face a huge impact force

to deposit onto the system. As a result, there is little nano-ZnO on the surface of the substrate material, and the hydrophobic performance of the coating decreases. With the increase in spraying distance, the movement time of the system under the atmospheric environment is prolonged, and the impact force on nanoparticles is reduced. Consequently, it is easier for nano-ZnO to deposit on the surface of the substrate with PTFE, and the hydrophobic performance of the coating is enhanced again.

The mass ratio of PTFE to nano-ZnO and the spraying distance affects not only the wettability of the coating but also the coating appearance and coating efficiency. Fig. 6. shows the appearance of the coatings at different mass ratios of PTFE to nano-ZnO at different spraying distances. When the mass ratio is 0:1, 1:1, 1:2, or 1:3, a layer of a water wave is observed on the coatings prepared at spraying distances of 0.1 and 0.2m. This can be attributed to the sagging phenomenon induced by the strong impact force during close-distance spraying. After the sagging liquor is dried, the water wave pattern is formed, affecting the homogeneity of coatings. In addition, when the mass ratio is 0:1, 1:1, 1:2, and 1:3, some coating surfaces show a cracking phenomenon. In coatings with low PTFE addition amount, high content of nano-powder can lead to high hardness and poor flexibility of coatings after drying, inducing cracks in coatings. With the increase in the additional amount of PTFE, the cracking is gradually improved. However, when the amount of PTFE is too high, the superhydrophobic performance of coatings decreases. Based on the above analysis, it can be deduced that when the mass ratio of PTFE to nano-ZnO is 4:1, the coating shows good superhydrophobic performance and stability.

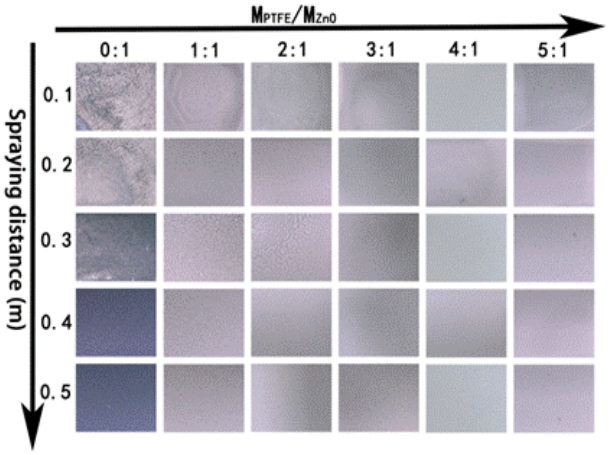

Fig. 6. The appearance of coatings at different mass ratios of PTFE to nano-ZnO at different spraying distances.

The influence of spraying distance is further discussed here. When the spraying distance is small, the coatings film is thick and the coating efficiency is high, however, the large impact force leads to poor hydrophobic performance. Long-distance spraying greatly reduces the coating efficiency and wastes a lot of coating, however, the surface granular sensation and porosity also increase significantly. Thus, the hydrophobic performance of coatings is greatly enhanced, the stability of the coatings is reduced. According to spraying practice, it is concluded that the spraying manner from near to far is the most suitable method. When the mass ratio of PTFE to

nano-ZnO is 4:1, a thick and homogenous surface is sprayed at a spraying distance of 0.1m firstly, and then the spraying gun slowly moves away from the surface to a spraying distance between 0.3 and 0.4m. During the away movement of the spraying gun, the spraying operation is not stopped. Thus, the coating surface has good stability, a beautiful and pleasant appearance, and desirable hydrophobic performance, and the coating efficiency is also improved. Fig. 7(a). shows the digital photo of liquid drops on the superhydrophobic coating. Fig. 7(b). shows the contact angles when water droplets of 8μL are dropped on aluminum substrate, PTFE coating, and ZnO@PTFE superhydrophobic coating. Fig. 7(c). reveals the images when a water droplet of 4μL approaches to, contacts with, and leaves from the nano-ZnO@PTFE superhydrophobic coating, respectively. The prepared ZnO@PTFE superhydrophobic coating has a smooth appearance, exhibits high contact angles and low viscous force between water droplets and the coating. Contact angles between the water droplet and pure Al substrate, PTFE coating, and nano-ZnO@PTFE superhydrophobic coating are 51.1°, 75.4°, and 165.3°, respectively.

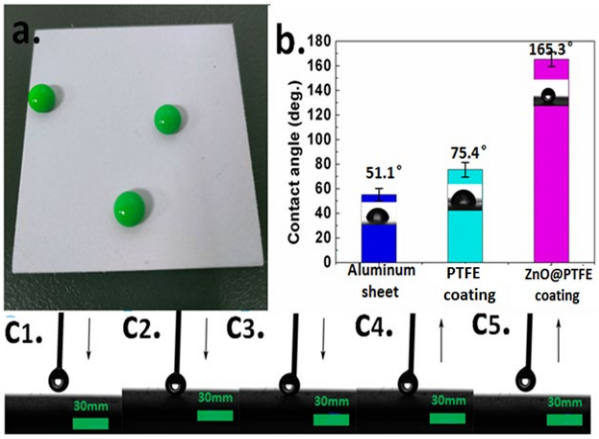

Fig. 7. (a) Digital photo of liquid drop on nano-ZnO@PTFE superhydrophobic coating. (b) contact angles of three different coatings. (c) images when a water droplet approaches to, contacts with, and leaves from the nano-ZnO@PTFE superhydrophobic coating.

3.3. Microscopic morphology analysis of the coatings

A rough structure is one of the necessary conditions to construct superhydrophobic coatings. Fig. 8. shows the SEM images of the coating at different magnifications. There are many tiny mastoid structures on the surface of the coating, and the surface structure is rough, conducive to improving the superhydrophobic performance. Moreover, the surface of the coating is compact, attributed to the compact structure formed by filling CNTs to the PTFE and nano-ZnO systems. However, some small holes are also observed in the coating, which may be caused by uneven spraying of the coating or too fast evaporation of the solution during oven drying. Fig. 8(d). shows the SEM image of the cross-section of the coating which is closely bonded to the surface of the substrate and has a thickness of about 100μm, with many nano-ZnO particles on the coating surface.

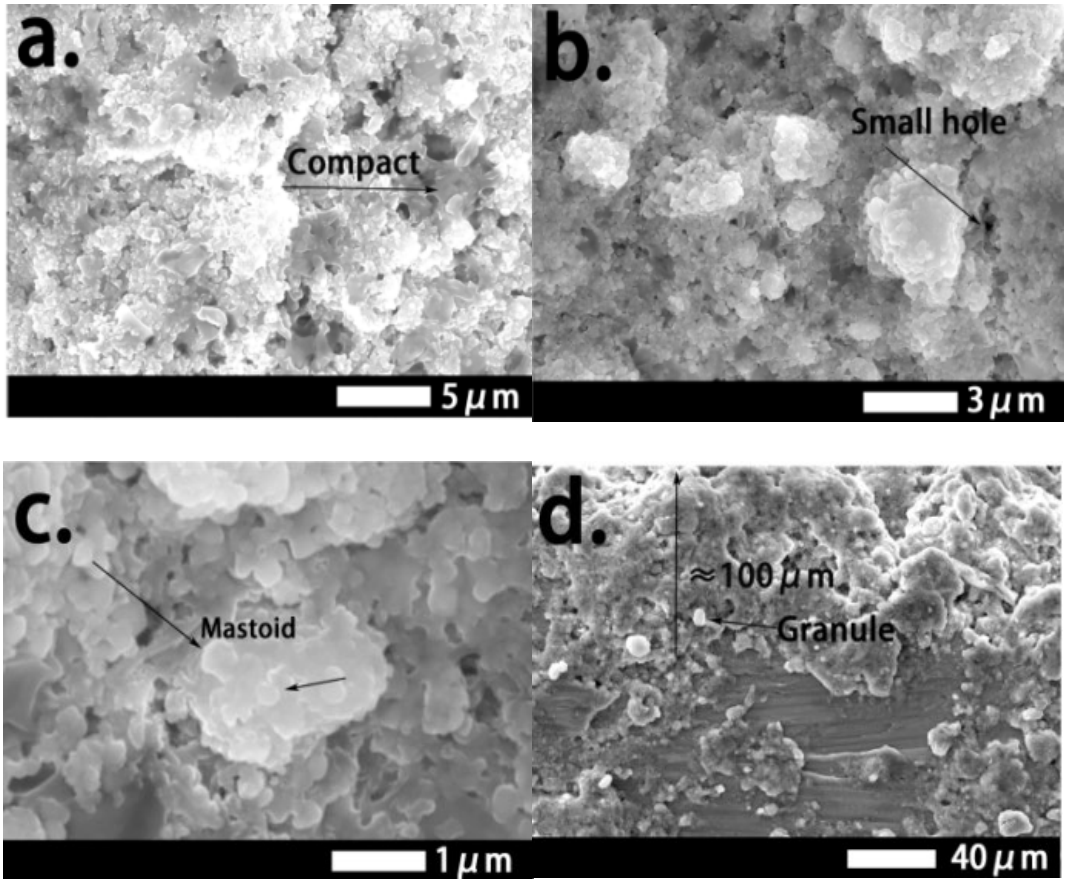

Fig. 8. SEM images of the microscopic morphology of nano-ZnO@PFTS at different magnifications. (a) 10,000×. (b) 30,000×. (c) 50,000×. and (d) 1,000× for the cross-section of the coating.

Coating surface evenness is one of the important factors to construct a homogenous coating. Fig. 9. shows the surface element distribution of the coating obtained by EDS mapping. The surface element distribution corresponds to the structure of ZnO@PTFE superhydrophobic coating, and each element is evenly distributed on the surface, confirming the homogenous surface structure of the coating.

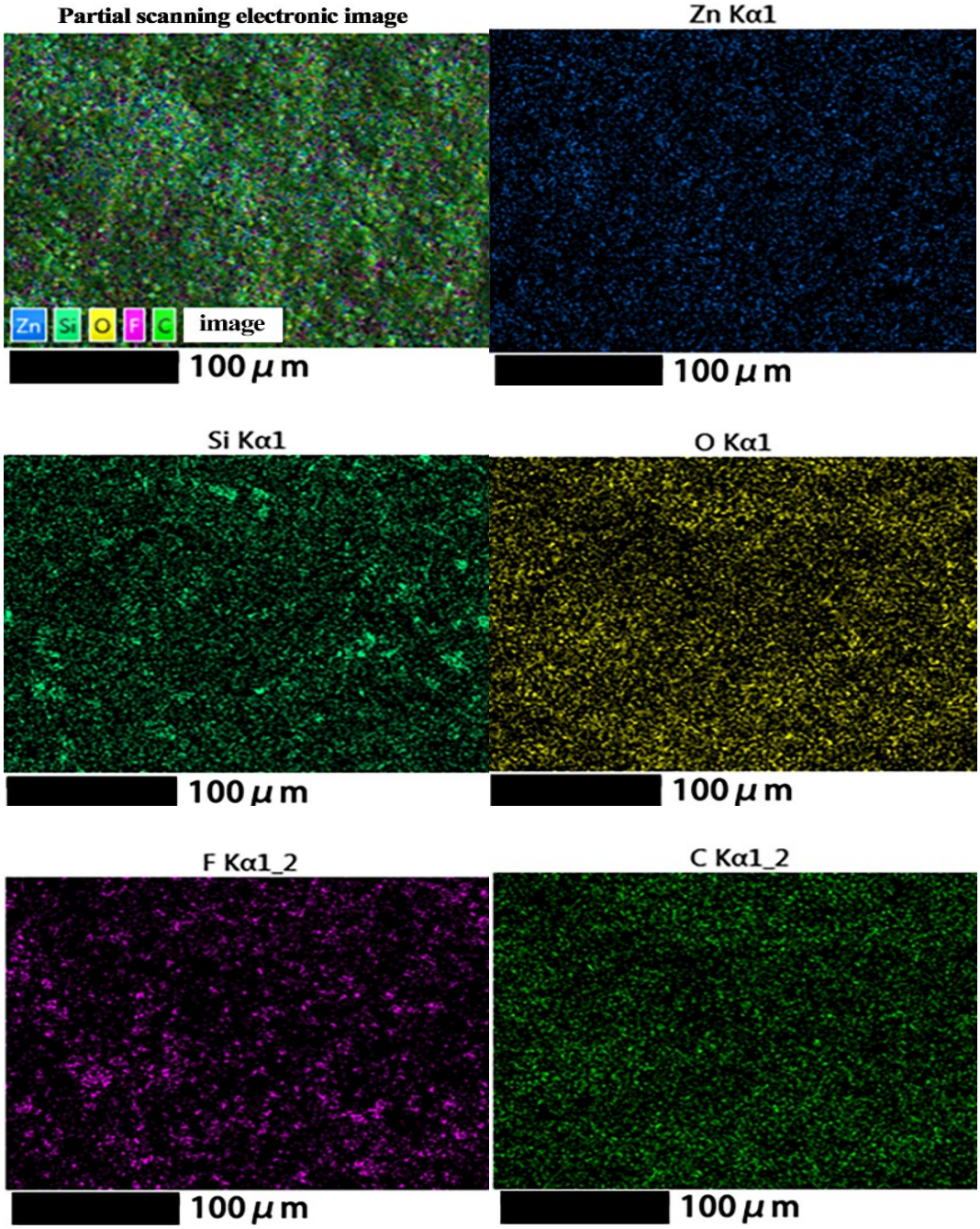

Fig. 9. EDS mapping results of the element distribution on the coating surface.

3.4. Mechanical stability of the coatings

Mechanical wear is one of the most common damage forms in daily life and is also one of the key factors in the practical application of superhydrophobic coatings. Since there is no specific evaluation standard to measure the mechanical durability of superhydrophobic coatings, the most commonly used sandpaper wear method is used in this test. Fig. 10(a). and (b) are the microscopic images under the stereoscopic microscope of ZnO@PTFE superhydrophobic coating, before and after friction. Fig. 10(b). shows wear marks on the surface of the coating and Fig. 10(c). indicates the dripping state of water droplets after the coating is worn by 4.0m. Water droplets still show a hydrophobic state on the coating surface after friction. Fig. 10(d). reveals the contact angle and

sliding angle of the coating, measured after each friction distance of 0.5m. The hydrophobic performance of the coating does not change much after the friction of 4.0m and the coating still exhibits superhydrophobicity. Fig. 10(e). shows three pictures taken from the dynamic video when a water droplet drops on the friction surface. The coating still has low viscous force after friction, and the water droplet does not stick to the surface after friction, indicating the superhydrophobicity and low viscous force after the wear test. Fig. 10(f1). and (f2) are SEM images of 500 times and 10,000 times, respectively, after the coating is worn. Although the surface layer of the coating is worn away, the internal powder particles are still closely bound to PFTS. The nano-ZnO particles are evenly distributed on the surface layer and inside the coating. These results indicate that the surface of the coating has a certain wear loss after friction, however, the superhydrophobicity of the surface is relatively stable.

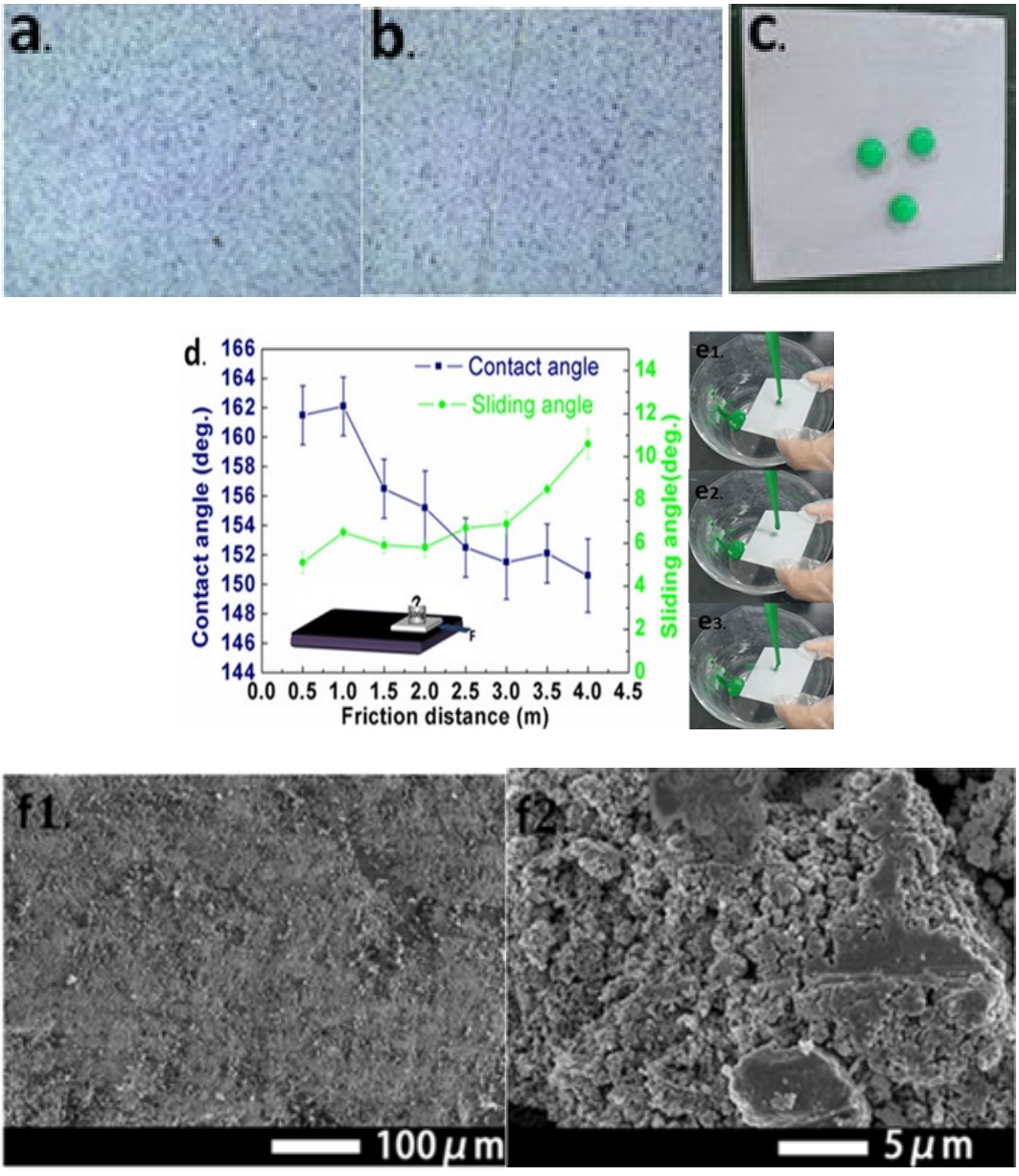

Fig. 10. Anti-friction performance test. (a) coating surface before friction. (b) coating surface after friction. (c) water droplet state on the coating surface after friction. (d) contact angle and sliding angle of the coating measured after each friction distance of 0.5 m. (e) screenshots from the dynamic video when a water droplet drops on the friction surface. (f) SEM images of the coating after friction.

3.5. Antibiosis performance analysis of the coatings

Bacterial adhesion in production and living brings a lot of hidden dangers to humans and it is an important part of dirt on the surface of materials. In this experiment, we selected common gram-negative Escherichia coli, gram-positive Staphylococcus aureus, and Candida albicans fungus to test the antibacterial performance of the coating.

3.5.1. Antibiosis performance of the coatings to Escherichia coli

Escherichia coli is widespread in the human gut. The LB nutrient agar medium is used for the antibacterial test, and results are shown in Table 1. and Fig. 11. The colonies grew on the culture medium of HDPE, PTFE coating, and 1060 aluminum sheet. According to the antibacterial formula, R=(B-A)/B×100%, the antibacterial rates of 1060 aluminum sheet and PTFE coating are 36.5% and 25.0%, respectively. In contrast, no colonies are observed on the culture medium incubated by ZnO@PTFE superhydrophobic coating, suggesting that the nano-ZnO@PTFE superhydrophobic coating has an excellent anti-adhesion effect on Escherichia coli.

Table 1. Antibiosis performance testing results of different samples for Escherichia coli.

Sample	Colony count	Antibiosis rate
Blank control (HDPE)	52	-
1060 aluminum sheet	33	36.5%
PTFE coating	39	25.0%
ZnO@PTFE superhydrophobic	0	99.9%
coating		

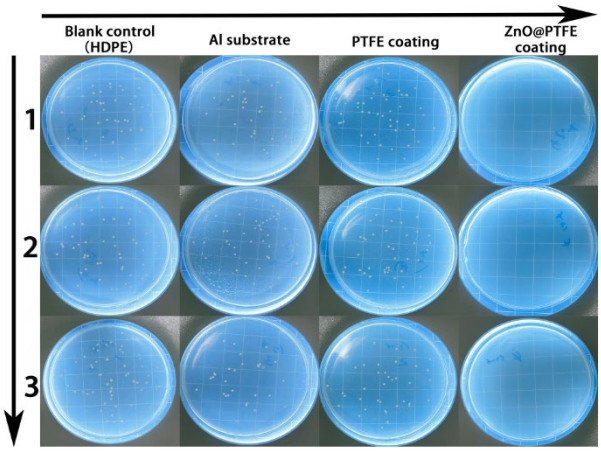

Fig. 11. Antibiosis performance testing results of different samples for Escherichia coli.

3.5.2. Antibiosis performance of the coatings to Staphylococcus aureus

Staphylococcus aureus is one of the most important pathogenic bacteria in human beings which can cause many serious infectious diseases. The LB nutrient agar medium is used for the antibacterial test, and results are shown in Table 2. and Fig. 12. There are massive bacterial

colonies on the culture media incubated by HDPE coating, PTFE coating, and 1060 aluminum sheet. According to the antibacterial formula, R=(B-A)/B×100%, the antibacterial rates of 1060 aluminum sheet and PTFE coating are 43.9% and 34.6%, respectively. In contrast, there are no colonies on the culture medium incubated by nano-ZnO@PTFE superhydrophobic coating, indicating that the nano-ZnO@PTFE superhydrophobic coating exhibits an excellent anti-adhesion effect on staphylococcus aureus.

Table 2. Antibiosis performance testing results of different samples for Staphylococcus aureus.

Sample	Colony count	Antibiosis rate
Blank control (HDPE)	387	-
1060 aluminum sheet	217	43.9%
PTFE coating	253	34.6%
ZnO@PTFE superhydrophobic coating	0	99.9%

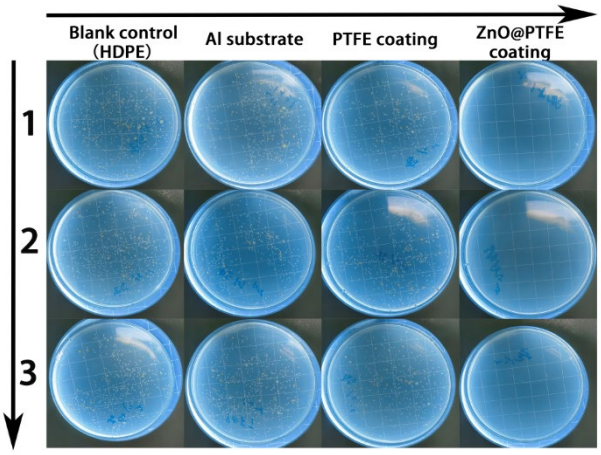

Fig. 12. Antibiosis performance testing results of different samples for Staphylococcus aureus.

3.5.3. Antibiosis performance of the coatings to Candida albicans

Candida albicans is a common fungus, widely existing in nature. The red Bengal agar culture medium is used for the antibacterial test, and results are shown in Table 3. and Fig. 13. There are dense white Candida albicans colonies overgrown on the culture medium incubated by HDPE coating, PTFE coating, and 1060 aluminum sheet. According to the antibacterial formula, R=(B-A)/B×100%, the antibacterial rates of 1060 aluminum sheet and PTFE coating are 31.1% and 38.2%, respectively. In contrast, no colonies are observed on the culture medium incubated by nano-ZnO@PTFE superhydrophobic coating, indicating that the nano-ZnO@PTFE superhydrophobic coating has an excellent anti-adhesion effect on Candida albicans. This is the combined result of the antibacterial effect of nano-ZnO and the superhydrophobic surface of the coating.

Table 3. Antibiosis performance testing results of different samples for Staphylococcus aureus.

Sample	Colony count	Antibiosis rate
Blank control (HDPE)	280	-
1060 aluminum sheet	193	31.1%
PTFE coating	173	38.2%
ZnO@PTFE superhydrophobic coating	0	99.9%

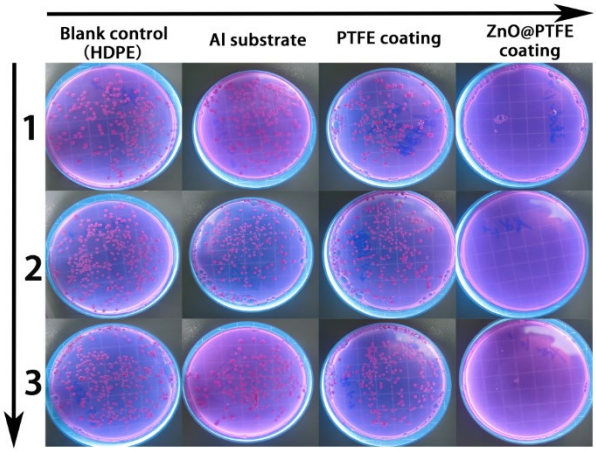

Fig. 13. Antibiosis performance testing results of different samples for candida albicans.

3.6. Antibacterial mechanism analysis

PTFE coating and 1060 aluminum sheet have a slight anti-adhesion effect, attributed to the low surface tension of PTFE and the bactericidal effect of aluminum ions on the surface of the 1060 aluminum sheet, while the nano-ZnO@PTFE superhydrophobic coating has an excellent anti-adhesion effect on three different types of bacteria. Fig. 14. reveals the schematic diagram of the anti-biological adhesion mechanism of nano-ZnO@PTFE superhydrophobic coating. The coating has a superhydrophobic surface, and extremely small water contact area and low adhesion force make it difficult for bacteria to approach the superhydrophobic surface. Moreover, nano-ZnO particles have a good antibiosis effect, which sufficiently reduces or even eliminates the biological adhesion to the coating surface.

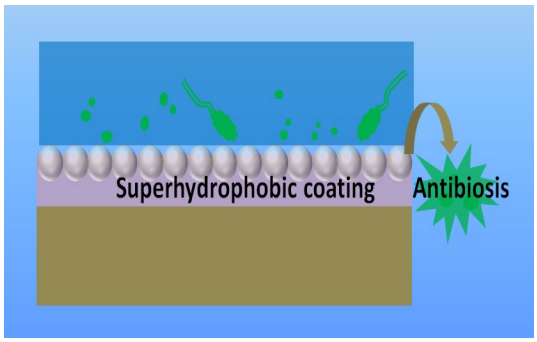

Fig. 14. Antibacterial mechanism of nano-ZnO@PTFE.

4. Conclusions

In this research, nano-ZnO@PTFE coating with superhydrophobic performance was prepared by a simple spraying process with blended nano-ZnO and PTFE. Fourier transform infrared spectroscopy (FTIR) and field emission scanning electron microscopy (FSEM) were used to characterize the coatings. The effect of the mass ratio of PTFE to nano-ZnO and the spraying distance on the morphology and wettability of coatings were investigated. The friction resistance of the coatings was measured and antibacterial properties of coatings for Escherichia coli, Staphylococcus aureus, and Candida albicans were tested. Obtained results showed that the optimal mass ratio of PTFE to nano-ZnO was 4:1 and that the optimal spraying method was spraying from near to far. SEM and EDS observation suggested the coating surface structure was compact, and the surface element distribution of the coating thickness was homogenous. The coating exhibited a thickness of about 100μm, and the substrate was closely bonded to the coating. After friction testing, the superhydrophobic performance of the coating surface was stable. Consequently, the coating showed excellent antibacterial performance. Our work provides a reference for the research and application of anti-biological adhesion of superhydrophobic coatings.

Acknowledgements

This work was supported by National Natural Science Foundation of China (52073127) and Changzhou Sci & Tech Program (CM20193004).

References

[1] F. Sahin, N. Celik, A. Ceylan, et al., Chemical Engineering Journal, 431 (2022) 133445; https://doi.org/10.1016/j.cej.2021.133445

[2] A. Ali, M.I. Jamil, J. Jiang, et al., Journal of Polymer Research, 27 (2020) 85; https://doi.org/10.1007/s10965-020-02054-z

[3] A. Mostafaei, F. Nasirpouri, Journal of Coatings Technology and Research, 10 (2013) 679-694;

https://doi.org/10.1007/s11998-013-9487-1

[4] Z. Hadzhieva, A. R. Boccaccini, Current Opinion in Biomedical Engineering, 21 (2022) 100367; https://doi.org/10.1016/j.cobme.2021.100367

[5] T. Wei, Y. Qu, Y. Zou, Y. Zhang, Q. Yu, Current Opinion in Chemical Engineering, 34 (2021) 100727; https://doi.org/10.1016/j.coche.2021.100727

[6] E. Sharifikolouei, Z. Najmi, A. Cochis, et al., Materials Today Bio, 12 (2021) 100148; https://doi.org/10.1016/j.mtbio.2021.100148

[7] H. Jin, L. Tian, W. Bing, et al., Progress in Materials Science, 124 (2022) 100889; https://doi.org/10.1016/j.pmatsci.2021.100889

[8] Z. He, X. Lan, Q. Hu, et al., Progress in Organic Coatings, 157 (2021) 106285; https://doi.org/10.1016/j.porgcoat.2021.106285

[9] E. Trávníčková, B. Pijáková, D. Marešová, L. Bláha, Journal of Environmental Chemical Engineering, 8 (2020) 104153; https://doi.org/10.1016/j.jece.2020.104153

[10] H. Khaleghi, A. Eshaghi, Surfaces and Interfaces, 20 (2020) 100559; https://doi.org/10.1016/j.surfin.2020.100559

[11] H. Li, S. Yu., Applied Surface Science, 420 (2017) 336-345; https://doi.org/10.1016/j.apsusc.2017.05.131

[12] T. Zhu, S. Li, J. Huang, M. Mihailiasa, Y. Lai, Materilas & Design, 134 (2017) 342-351; https://doi.org/10.1016/j.matdes.2017.08.071

[13] T. Xiang, Y. Han, Z. Guo, R. Wang, S. Zheng, S. Li, C. Li, X. Dai, ACS Sustainable Chemistry & Engineering, 6 (2018) 5598-5606; https://doi.org/10.1021/acssuschemeng.8b00639

[14] Y. C. Liu, W. J. Huang, S. H. Wu, M. Lee, J. M. Yeh, H. H. Chen, Corrosion Science, 138 (2018) 1-7; https://doi.org/10.1016/j.corsci.2018.03.044

[15] P. Varshney, J. Lomga, P. K. Gupta, S. S. Mohapatra, A. Kumar, Tribology International, 119 (2018) 38-44; https://doi.org/10.1016/j.triboint.2017.10.033

[16] S. Bengaluru Subramanyam, V. Kondrashov, J. Ruhe, K. K. Varanasi, ACS Applied Materials & Interfaces, 8 (2016) 12583-12587; https://doi.org/10.1021/acsami.6b01133

[17] Huang. W, Huang. J, Guo. Z, Liu. W., Advance in Colloid and Interface Science, 304 (2022) 102658; https://doi.org/10.1016/j.cis.2022.102658

[18] J. H. Chu, G. X. Sun, L. B. Tong, Z. H. Jiang, Colloids and Surfaces A: Physicochemical and Engineering Aspects, 617 (2021) 126370; https://doi.org/10.1016/j.colsurfa.2021.126370

[19] A. Tombesi, S. Li, S. Sathasivam, K. Page, et al., Scientific Reports, 9 (2019) 7549; https://doi.org/10.1038/s41598-019-43386-1

[20] Y. Hu, X. Ma, H. Bi, J. Sun, Colloids and Surfaces A: Physicochemical and Engineering Aspects, 603 (2020) 125227; https://doi.org/10.1016/j.colsurfa.2020.125227

[21] V. S. Saji, Advances in Colloid and Interface Science, 283 (2020) 102245; https://doi.org/10.1016/j.cis.2020.102245

[22] S. Mallakpour, V. Behranvand, European Polymer Journal, 84 (2016) 377-403; https://doi.org/10.1016/j.eurpolymj.2016.09.028

[23] D. Chopra, K. Gulati, S. Ivanovski, Materials Today Advances, 12 (2021) 100176; https://doi.org/10.1016/j.mtadv.2021.100176

[24] A. Bansal, J. Singh, H. Singh, D. K. Goyal, Wear, 477 (2021) 203886; https://doi.org/10.1016/j.wear.2021.203886

[25] M. I. Rahmah, R. S. Sabry, W. J. Aziz, Journal of Bionic Engineering, 19 (2022) 139-154; https://doi.org/10.1007/s42235-021-00106-8

[26] M. Haji-Savameri, A. Irannejad, S. Norouzi-Apourvari, et al, Scientific Reports, 12 (2022) 17059; https://doi.org/10.1038/s41598-022-20729-z